CHARACTERIZATION FACILITY FOR NDE TRANSDUCERS

K. M. Lakin
University of Southern California
Los Angeles, California

ABSTRACT

The characterization of NDE transducers involves an assessment of the bidirectional acousto-electric conversion between electrical and acoustic terminals and an evaluation of the near and far-field radiation patterns. The internal details of the transducer are largely unknown and, consequently, the traditional techniques for analyzing the structures cannot be applied. Instead, the transducer may be characterized as a hybrid two-port network whose parameters may be determined by relatively simple measurements taken at the electrical port when the acoustic loads are known. The radiation pattern involves measurement only in the region exterior to the transducer. There are several techniques which may be used to accomplish this task. Our approach has been to measure the acoustic field in the far-field region and then to reconstruct the field at the face of the transducer. Once we have the field at the transducer, an evaluation of the source may be readily determined from amplitude and phase contour plots or from gray scale or pseudo-color images.

Introduction

The characterization of NDE transducers is a problem which could be greatly aided by determining the fields at the surface of the transducers. Such information would be useful not only for directly characterizing the transducer, but also as a check on the predictions of theoretical models of the transducers.[1] The fields at the surface of the transducer or in any intermediate plane can be reconstructed from measurements of the amplitude and phase of the radiation pattern. This measurement and reconstruction process is basically holography.[2]

Previous attempts at reconstructing images of acoustic radiators or scatterers have involved recording the radiation pattern on film and reconstructing the image optically.[3] Such recordings are Gabor or on-axis holograms. As such, the reconstructed image is degraded by a second defocused image of the object superimposed on the desired image. In the work done here, the radiation pattern is scanned and the resultant data is processed with a digital computer to generate an image free of any degrading secondary images.

The total system consists of an analog electronic recording system, A/D conversion, and digital processing. The transducer is placed in water and driven with a constant frequency (5 MHz) signal. A second transducer scans the radiation pattern measuring amplitude and phase. Here an oscillator (5 MHz) is used as a reference signal in order to extract the phase. The data points are recorded in the Fresnel diffraction zone. By multiplying the data with a quadratic phase term, we obtain the equivalent of the Fraunhofer diffraction pattern.[1] The data are also multiplied with an apodizing factor which will be discussed later. Given the Fraunhofer diffraction pattern, the fields at the surface of the transducer are found by taking the inverse Fourier transforms of the data.[1] These steps can be better visualized by looking at a totally optical analog of this system as shown in Fig. 1. Multiplying with a quadratic phase factor in (a) is equivalent to placing a collimating lens in the scanning plane. The discrete Fourier transform (DFT) has its parallel in the second lens. It is well known that the field in the back focal plane of a lens is equal to the Fourier transform of the field present in the front focal plane.[4] Thus lens L2 performs a Fourier transform of the radiation pattern. The combination of collimating lens L1 and Fourier transform lens L2 is seen to form a simple imaging system which images the transducer.

Apodization

If one takes all the data points in the Fourier plane, weights them equally, and then does the inverse Fourier transform, the resultant image exhibits ringing at any sharp edges. This is a manifestation of the Gibb's overshoot phenomenon associated with truncating Fourier series. This effect can be minimized without significant loss of resolution by applying appropriate weignts to the data points. This is equivalent to placing an apodization filter in the optical system of Fig. 1. A test was made to compare several different apodization functions. For the test, a square pulse was used. The pulse function was Fourier transformed (digitally), the resultant spatial frequency samples were multiplied with the apodization function, and then an inverse Fourier transform was performed (again digitally). Figure 2 shows the results of this procedure for several different apodization functions. On the scale of these plots, the square input function had a width of 32. The heights have been normalized to 200. Figure 2(a) shows the ringing that results when no apodization is used. Four cases were then evaluated (Figs. 2(b) - 2(e)). The last three cases (Figs. 2(c) - 2(e)) all give very good and approximately equivalent results. These filters respectively have the forms: Gaussian, A+cosine, and sin(x)/x. Figure 3 shows reconstructions of the intensity on the surface of a transducer with and without apodization. The smoothing of the overshoot on the edges is apparent.

Although the apodization, in principle, does not result in any information loss, it does result in an effective signal loss. Thus the three above-mentioned apodization filters which gave essentially equivalent results under noise-free conditions, may perform differently in the presence of noise.

Aspects of the Imaging System

Distortion - In general, an imaging system will introduce depth distortion in the image of a three-dimensional object. The longitudinal magnification, M, of a single lens imaging system is a nonlinear function of position along the axis of the system. If one wishes to image curved surfaces without longitudinal distortion, one must carefully choose the imaging system. Figure 4 shows a telecentric imaging system for which the longitudinal magnification is a constant $M = f2/f1$, where f1 and f2 are the focal lengths of the two lenses L1 and L2. For the imaging system used in this project (see Fig. 1) the longitudinal magnification is, in general, not constant.

$$M = f1.f2/[x1(f2 - f1) + f1]^2 \qquad (1)$$

Here, f1 and f2 are again the focal lengths of the lenses and x1 is the distance of the object plane from the front focal plane of lens L1. We note, however, that if $f1 = f2$, the longitudinal magnification becomes a constant, in fact, unity. So for the particular case, the system shown in Fig. 1 gives distortion-free imaging at unit magnification.

Depth distortion is only a problem when one considers displaying three-dimensional data. Of the three-dimensional display techniques discussed later, depth distortion affects primarily the optical holographic technique.

Lateral Distortion - In the work done thus far, the collected data has been multiplied with a quadratic phase factor before being Fourier transformed (Fig. 1). The effect of this phase factor is analogous to that of a collimating lens. The quadratic phase factor is an approximation to the ideal phase correction. The approximation is only valid for paraxial rays, or in other words, when the dimensions of the scanned area and of the imaged area are small compared to the distance between the object plane and the scan plane. Since the computer has replaced the lens, it is possible to improve this approximation so that the only remaining restriction is that the object field must be small in terms of the solid angle it subtends at the measurement plane. The size of the measurement plane itself is unrestricted.

This relaxation of the restrictions on the system is achieved by using the exact phase factor for imaging a point source as predicted by Huygen's theory. This new phase factor constitutes an "ideal lens" for a point source located on the axis. This ideal lens is simply a spherical phase;

$$\phi(x,y) = 2\pi/\lambda \sqrt{x^2 + y^2 + R^2}\ , \qquad (2)$$

where λ is the wavelength of radiation in the given medium (e.g., water), x,y are the coordinates in the measurement plane, and R is the distance from the point source to the measurement plane. This exact phase factor can be used instead of its paraxial approximation in Fig. 1.

$$\phi'(x,y) = \frac{\pi}{\lambda}\left(\frac{x^2+y^2}{R}\right) + \text{constant} \quad \text{if } R \gg (x^2+y^2). \quad (3)$$

Although the new solution is only exact for the point on axis, it also reduces the distortion in the images of off-axis points.

Three-Dimensional Presentation

A major concern of this program is the visualization of an ultrasound transducer or scatterer. In particular, a means of presenting any three-dimensional structure of the source is important. There are several possible ways of displaying three-dimensional information that have been studied in regard to this project. These methods are described below.

Optical Holographic Reconstruction - This method involves the creation of a hologram from the recorded data. This hologram could then be reconstructed optically to give an exact three-dimensional image of the original source. This would be an ultimate presentation in terms of the amount of information in the display. Virtually all of the available three-dimensional information is retained. However, this is an extremely involved process. The recorded data must be converted into an optical hologram. The amplitude information recorded in the Fresnel zone can be converted to a transparency by means of a plotting microdensitometer. The phase information is more difficult. To get the phase directly, we have to record an intensity related to the phase on film, and then bleach the film to convert the intensity variations to phase variations. Such a phase recording combined with the previously mentioned amplitude transparency produces an on-axis phase-and-amplitude hologram. Alternatively, the phase could be encoded as intensity variations by "interfering" the phase front with a reference phase front and recording the resulting fringe pattern. This could be used to produce an off-axis type of hologram. Although the off-axis approach avoids the problems associated with bleaching film to create a phase record, it requires a higher spatial resolution on the phase record; thus, it puts more severe requirements on the plotting microdensitometer.

Another problem with the holographic display approach is that the data tends to cover an extremely large dynamic range (see Fig. 5). Computer holograms, however, are only capable of recording fairly small dynamic range objects. A number of techniques were explored to overcome this difficulty. One such technique was an iterative technique whereby the object was first reconstructed digitally, then a random phase was imposed on the reconstruction. This was Fourier transformed to get a first approximation to the desired hologram. In this hologram the phase information was retained but the amplitude was set equal to some predetermined function with low dynamic range requirements. Both a constant function and a Gaussian function were used in this regard. From this modified Fourier transform, a reconstruction was made. Here also the phase was retained, but the amplitude was set equal to the original amplitude in the reconstruction. This process was repeated after each Fourier transform, setting the amplitude equal to the predetermined values, until a hologram was obtained whose amplitude deviated only slightly from the desired function. This technique was successful, particularly when the Gaussian amplitude was applied to the holograms. However, it is time-consuming and, furthermore, is only suitable for planar or nearly planar objects. The resultant holograms are shown in Fig. 6. It should be noted that all of these holograms are of the Lohmann type.[5] The amplitude of the field is encoded through a type of pulse width modulation while the phase is encoded through pulse position modulation.

A second method consisted of digitally precompensating the data to reduce its dynamic range. This could be done, for instance, by multiplying it with an appropriately scaled inverse Gaussian. A hologram was generated from this compensated data. Then upon reconstruction, the hologram was illuminated with a nonuniform beam which restored the original dynamic range. If the compensation function was an inverse Gaussian, which proved most practical, the natural Gaussian profile of a laser beam in the TEM mode could be used to illuminate the hologram. The main problem with this technique is that there are strict alignment requirements in the reconstruction stage.

A third technique of avoiding the dynamic range problem promised to overcome some of the difficulties of the other two, but lack of time prevented its thorough investigation during this project. In this approach, an arbitrary plane near the object is reconstructed digitally. From this reconstruction an image plane hologram is generated. By recording in the image plane, the problem of extremely large dynamic range signals are avoided. The image plane hologram is then viewed through a coherent spatial filtering imaging system to convert the interference fringe information into phase information. Figure 7 shows a preliminary version of an image plane computer-generated hologram. For practical utilization a higher carrier frequency would be desirable. This approach is suitable for arbitrary three-dimensional objects and does not have the severe alignment problems of the previously mentioned technique.

Digital Reconstruction of Individual Planes - By multiplying the data with a given quadratic phase factor and performing a digital Fourier transform (DFT), we obtain an image of a given plane. The position of this plane along the "viewing axis" is determined by the quadratic phase factor. Thus by varying this phase factor we can scan through the depth of the object. By imaging several such planes we obtain a three-dimensional picture of the object in layers. Although this is the simplest method to implement, it gives the least satisfying presentation of information. Each contains an in-focus image of the section of the object which lies in that particular plane, but also all other planes are in the picture but out of focus. This method is computationally time-consuming if several planes are to be imaged.

One particular instance arose during the project in which this approach did prove quite useful, suggesting an important potential in evaluating transducers. A focused transducer was used as a test object. Since we have the capability of imaging any plane, it is possible to search for the focal plane of the transducer. This not only allows one to determine accurately and easily the focal plane from just one set of measurements, but it also allows one to measure the performance of the transducer by examining the quality of the point image in the focal plane. Figure 8 shows plots of the field intensity in various planes in front of a focused transducer.

Stereo Imaging - In this approach the measured data is used to generate a stereo pair of images. Stereo imaging is a simple means of conveying a large amount of information about an object. Stereo imaging has received renewed attention as a research subject in recent years.[6] To generate the stereo pair the recorded data is split into two groups; all data points recorded to the left of an imaginary center line being grouped in the "left hologram" and the points lying to the right of the line going into the "right hologram." Each hologram is used to generate an image of the object by means of a DFT. The two images form a stereo pair. The appropriate viewing system allows the observer to see a three-dimensional image. This approach has several advantages. It is considerably easier to implement than the optical holography approach. It is computationally preferable to the strictly digital method described above since it requires only two DFT's. It also gives a presentation that is easily digested by the human observer. The necessary software has been developed for this approach. A means of simultaneously displaying the two stereo images in the form of a green and a red image has been developed. These images can then be viewed through anaglyph glasses for a stereo image. Experiments on test data have demonstrated the feasibilities of this approach.

Phase Contours - The above techniques are well suited to displaying depth information of a few wavelengths or more. However, for variations of a wavelength or less, another approach is much more fruitful. This method consists of displaying contours of constant phase. Preliminary results in this area are very promising. Figure 9 is a picture of the reconstructed phase at the surface of a focused transducer. The surface is approximately spherical with a depth variation of about one wavelength (.03 cm). The phase variations are recorded here as intensity variations. The vertical fringe system is due to the fact that the transducer was tilted slightly, producing a linear phase variation across the face of the transducer. The curvature of the fringes indicates the spherical curvature of the transducer face.

Acknowledgements

The authors wish to thank Mr. A. Hsueh for his part in developing much of the software used in this work. Professor A. Sawchuk is also to be thanked for many helpful discussions and suggestions during the course of this project.

This research was sponsored by the Center for Advanced NDE operated by the Science Center, Rockwell International, for the Advanced Research Projects Agency and the Air Force Materials Laboratory under contract F33615-74-C-5180.

References

1. K. Lakin and A. Fedotowsky, IEEE Transactions Sonics and Ultrasonics, SU-23, 317 (1976).

2. B. P. Hildebrand and B. B. Brendon, Introduction to Acoustic Holography, Plenum Press, New York, 1972.

3. K. Preston, Jr., and Kreuzer, Applied Physics Letters, 10, 150 (1967).

4. J. W. Goodman, Introduction to Fourier Optics, McGraw-Hill, New York, 1968.

5. A. W. Lohmann and D. P. Paris, Appl. Opt., 6, 1739 (1967).

6. A. A. Sawchuk and H. C. Andrews, J. Opt. Soc. America, 66, 1111 (1976).

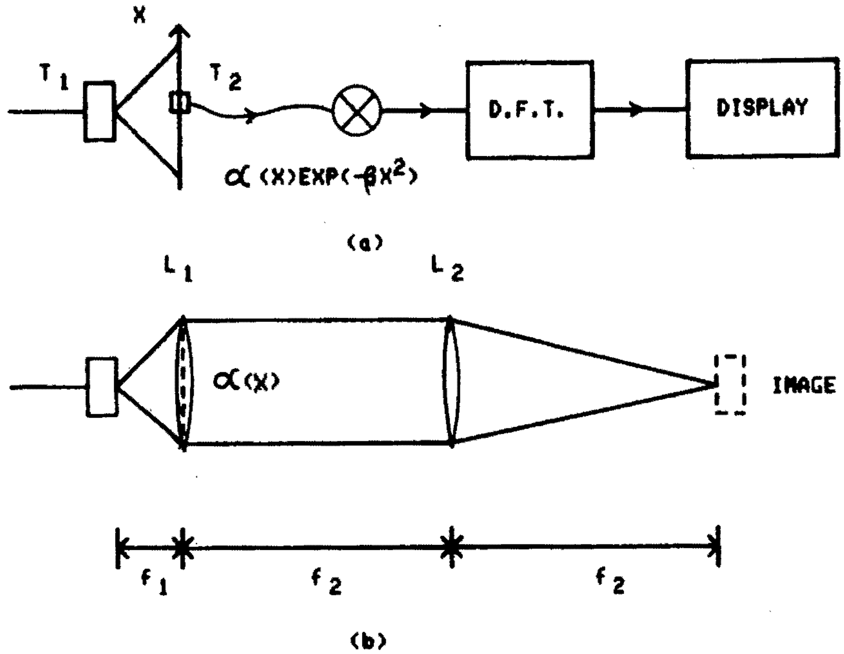

Figure 1. Digital imaging system: (a) Actual system. T_1 is the acoustic transducer being studied, T_2 is a transducer used as a scanning detector, $\alpha(x)$ is the apodization factor, $epx(-i\beta x^2)$ is the quadratic phase factor, D.F.T. represents a discrete Fourier transform; (b) Optical analog to the system shown in (a). L_1 is a collimating lens which corresponds to the quadratic phase factor, $\alpha(x)$ is the apodizing filter, and L_2 is a Fourier transforming lens. f_1 and f_2 are the focal lengths of L_1 and L_2, respectively.

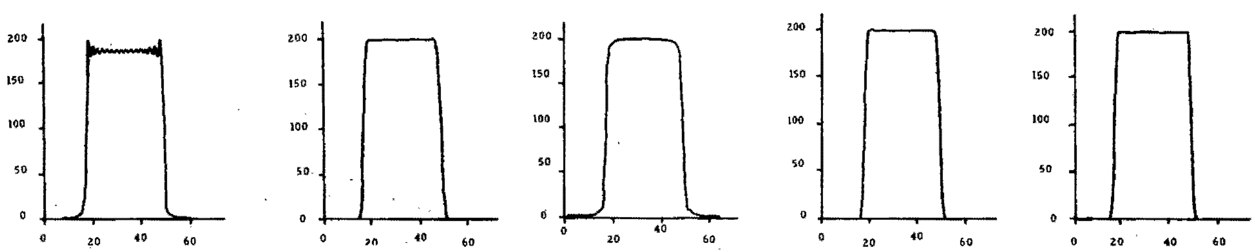

(a) Without apodization.
(b) Triangle function apodization.
(c) Gaussian apodization.
(d) (A+Cosine) apodization.
(e) Sinc function apodization.

Figure 2. Effect of apodization. A test object consisting of a square pulse was low-pass filtered with various apodization filters to eliminate ringing.

(a) No apodization, grey scale images of amplitude.

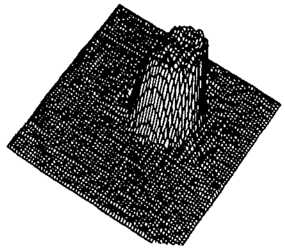

(b) No apodization, perspective plot of amplitudes.

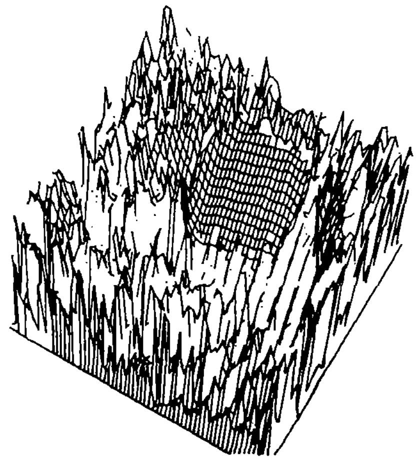

(c) No apodization, perspective plot of phase.

(d) Reconstruction of a transducer with apodization.

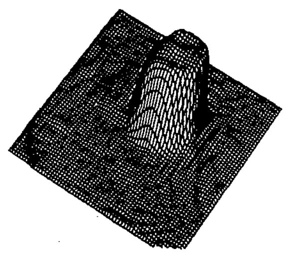

(e) With apodization, perspective plot of amplitude.

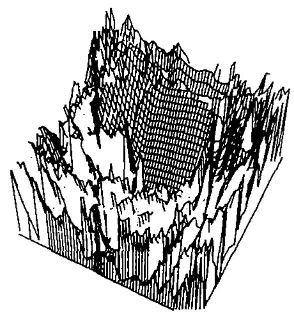

(f) With apodization, perspective plot of phase.

Figure 3. Effects of apodization on reconstruction of a transducer's amplitude and phase.

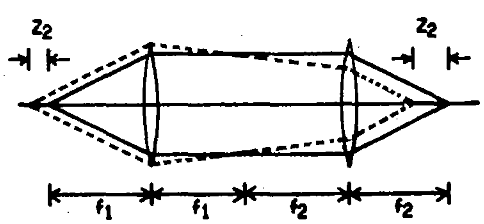

Figure 4. Telecentric imaging system. f_1 and f_2 are the focal lengths of lenses L_1 and L_2, respectively. For this system, displacements along the optical axis are imaged without distortion, i.e., $z_2 = (f_2/f_1)z_1$.

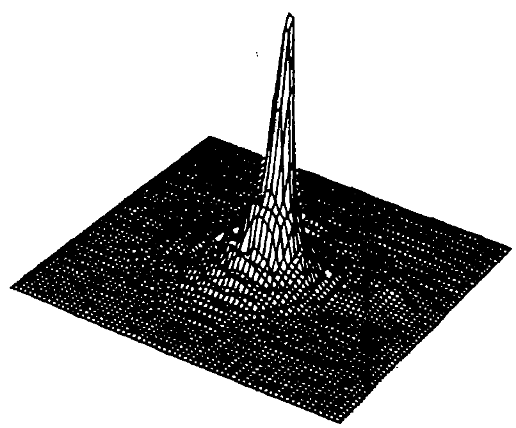

Figure 5. Plot of the field amplitude in the measurement plane.

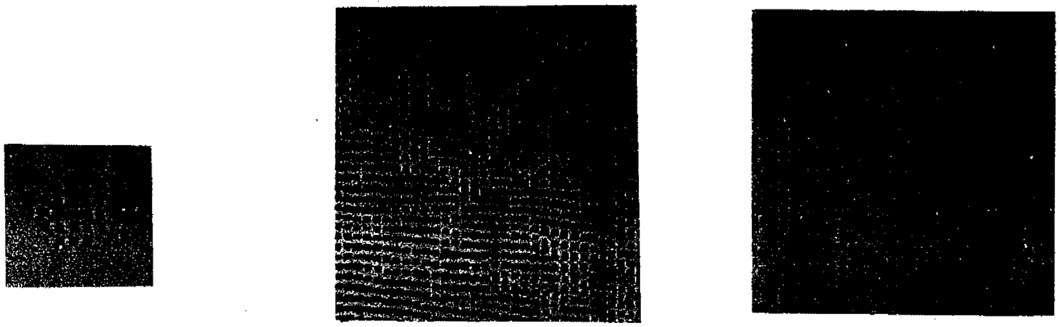

(a) Uncompensated hologram. Limited dynamic range of the plotting system causes only the central peak to be plotted.

(b) Compensated hologram. Amplitude has been forced to be approximately constant by the iterative method.

(c) Compensated hologram. Amplitude has been forced to approximate a Gaussian by the iterative method.

Figure 6. Binary computer-generated holograms of the data.

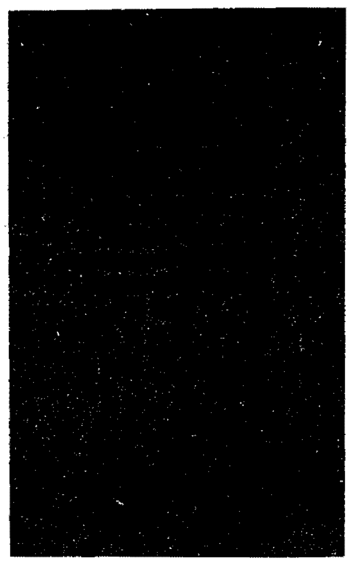

Figure 7. Binary computer-generated image-plane hologram.

(a) Image of the transducer surface.

(b) Image of a plane 9.6 cm in front of the transducer.

(c) Image of a plane 21.6 cm in front of the transducer. This is approximately the focal plane.

(d) Image of a plane 30.2 cm in front of the transducer.

Figure 8. Images of various planes in front of a focused transducer.

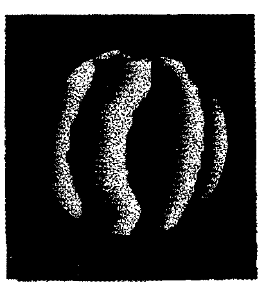

Figure 9. Phase contours on the surface of a focused transducer. Each intensity represents a constant phase. The fringes are due to a slight tilt of the transducer causing a linear phase variation across the face of the transducer.